SQUIRMER MODEL OF MICROSWIMMERS

MARTIN MURKO

Fakulteta za matematiko in fiziko
Univerza v Ljubljani

The study of microswimmers in low Reynolds number environments plays a crucial role in the understanding of biological locomotion. This article investigates the hydrodynamics governing microscale swimming, with a focus on the squirmer model – a canonical representation of self-propulsion driven by surface distortions. It begins with an overview of the fundamental principles of low Reynolds number hydrodynamics, including the Stokes equation and key concepts such as rate independence and the scallop theorem. The squirmer model is then derived, and its swimming velocity is calculated using both direct solutions of the flow field and the Lorentz reciprocal theorem. Squirmers are further classified into pushers and pullers according to their flow field characteristics, and their interactions with solid boundaries are examined. Theoretical predictions are finally compared with experimental data for *Volvox carteri*, demonstrating the model's effectiveness in capturing the behaviour of biological swimmers.

MODEL ZVIJAČA ZA MIKROPLAVALCE

Študij mikroplavalcev v okolju z nizkim Reynoldsovim številom ima ključno vlogo pri razumevanju biološkega samopogona. Članek obravnava hidrodinamiko, ki določa gibanje na mikroskali, s poudarkom na modelu zvijača (angl. *squirmer*), kanoničnem opisu samopogona, ki izhaja iz površinskih deformacij. Članek začne s pregledom temeljnih načel hidrodinamike pri nizkem Reynoldsovem številu, vključno s Stokesovo enačbo ter ključnimi pojmi, kot sta neodvisnost od hitrosti in teorem školjke. Nato je izpeljan model zvijača, njegova hitrost plavanja pa izračunana z uporabo neposrednih rešitev tokovnega polja ter Lorentzovega izreka o recipročnosti. Zvijači so nadalje razvrščeni na potiskače in vlečnike glede na značilnosti njihovih tokovnih polj, pri čemer so analizirane tudi njihove interakcije s togimi mejami. Teoretične napovedi so na koncu primerjane z eksperimentalnimi podatki za *Volvox carteri*, kar potrjuje učinkovitost modela pri opisu obnašanja bioloških plavalcev.

1. Introduction

At small scales, from 1 μm to 100 μm, which we can call the microscale, locomotion plays a decisive role in biological systems and also in artificial microswimmers. On the microscale, the fluid dynamics around swimmers differ fundamentally from macroscopic swimming due to the dominance of viscous forces. The Reynolds number, which quantifies the relative importance of inertial and viscous effects, is extraordinarily small in microorganisms, leading to unique swimming strategies. One of the most influential insights into swimming at low Reynolds numbers came from Purcell in the form of the scallop theorem, which states that time-reversible motion in a Stokes fluid cannot generate net propulsion [1]. Consequently, microswimmers must move with non-reciprocal patterns, such as fluctuating flagella, rotating helices, or surface distortions. A simple but powerful model for such motions is the squirmer model, introduced by Lighthill and Blake [2, 3]. The squirmer represents a spherical microswimmer that propels itself by tangential surface velocities, mimicking ciliated microorganisms such as volvox or paramecium. The model enables analytical and numerical investigations of self-propulsion, fluid interactions, and boundary effects. In this article, we first give an overview of the fundamental hydrodynamics governing swimming at low Reynolds numbers and the mathematical formulation of the squirmer model. Then we derive its swimming behaviour velocity using two approaches: direct solutions of the Stokes equation and the Lorentz's reciprocal theorem [4]. Furthermore, we classify squirmers as pushers or pullers based on their flow properties and study their interactions with solid boundaries. Finally, we compare the theoretical predictions with experimental observations of *Volvox carteri*, to illustrate the applicability of the model to microswimmers in the real world [5].

2. Low Reynolds number hydrodynamics

2.1 General properties

To understand the effect of the forces acting on a floating organism in an incompressible Newtonian fluid, we need to solve the Navier-Stokes equation for the velocity field $\boldsymbol{v}$, the density ρ and the viscosity $\boldsymbol{\eta}$

$$\rho\left(\frac{\partial}{\partial t}+\boldsymbol{v}\cdot\nabla\right)\boldsymbol{v}=-\nabla p+\eta\nabla^2\boldsymbol{v},\qquad \nabla\cdot\boldsymbol{v}=0, \tag{1}$$

where $\nabla\cdot\boldsymbol{v}=0$ only applies to incompressible fluids. The Navier-Stokes equation can be derived from the linear Cauchy momentum equation [6]. A Newtonian fluid is a fluid in which the relationship between the viscous part of the stress tensor and the strain rate tensor v_{ik} is linear. For incompressible fluids, the viscous part of the stress reads $\sigma^v_{ik}=2\eta v_{ik}$, where $v_{ik}=\frac{1}{2}\left(\partial_i v_k+\partial_k v_i\right)$, and

$$\sigma_{ik}=-p\delta_{ik}+\sigma^v_{ik}. \tag{2}$$

In order to solve Equation (1), we need sufficient boundary conditions. Normally we say that the velocity field at the boundary of the immersed body is zero, $\boldsymbol{v}|_{\partial B}=0$ (so-called no-slip boundary condition). The condition of incompressibility, $\nabla\cdot\boldsymbol{v}=0$, follows from the continuity equation. Since there are five variables in the general Navier-Stokes equation (three spatial components of $\boldsymbol{v}$, η and p), we need an additional equation, a thermodynamic relation $p=p(\rho)$. Once we have solved $\boldsymbol{v}$ and p, the stress tensor is given by Equation (2) and the force $\boldsymbol{F}$ and torque $\boldsymbol{M}$ acting on a submerged body are determined by integrating over its surface:

$$\boldsymbol{F}=\oint_{\partial V}\boldsymbol{\sigma}\cdot\boldsymbol{n}\,\mathrm{d}S,\quad \boldsymbol{M}=\oint_{\partial V}\boldsymbol{r}\times(\boldsymbol{\sigma}\cdot\boldsymbol{n})\,\mathrm{d}S. \tag{3}$$

If we convert the Navier-Stokes equation into a non-dimensional form, we find that the solution is parameterized with three constants: the Strouhal number, the Euler number, and the Reynolds number. The most important one for us is the Reynolds number, $Re=\frac{\rho VL}{\eta}$ where V is the typical velocity of the flow and L is the characteristic size of the swimming body. The Reynolds number indicates the properties of the flow regime and has several different physical interpretations.

- Consider a body of size L with steady surrounding flow with velocity V. Reynolds number is the ratio of the typical inertial term in the Navier-Stokes equation $\rho\boldsymbol{v}\cdot\nabla\boldsymbol{v}$, to the viscous forces per unit volume $\eta\nabla^2\boldsymbol{v}$. Thus, $Re=\rho VL/\eta$. In a low Reynolds number flow, the viscous forces dominate [7].

- The typical time scale for a local velocity perturbation to be convectively (by an inertial term) transported by the flow along a body is $t_{\text{conv}}=L/V$. On the other hand, the typical time for the perturbation to diffuse away from the body due to viscosity is $t_{\text{diff}}=\rho L^2/\eta$. Reynolds number is therefore $Re=t_{\text{diff}}/t_{\text{conv}}$, and low Reynolds number flow is the one for which fluid transport is dominated by viscous diffusion [7].

- Familiar interpretation is the definition with ratios of forces acting on the body. A typical viscous stress on a body is given by $\boldsymbol{\sigma}_{\text{viscous}}=\eta V/L$, leading to a typical viscous force $f_{\text{visc}}=\eta VL$. Inertial forces can be approximated from the Bernoulli equation $f_{\text{inert}}=\rho V^2L^2$. Similarly, Reynolds number is interpreted as $Re=f_{\text{inert}}/f_{\text{visc}}$, meaning that in low Reynolds effect of inertial forces is insignificant [7].

With these interpretations of the Reynolds number, we can determine the Reynolds number for certain microswimmers. For example, the bacterium *E. coli* ($L\approx 1-10\,\mu$m) with a velocity

$V \approx 10\,\mu\text{m s}^{-1}$ in water ($\rho \approx 10^3$ kg m^{-3}, $\eta = 10^{-3}$ Pa s) has a Reynolds number $Re \approx 10^{-5} - 10^{-4}$, a human spermatozoon with $V \approx 200\,\mu\text{m s}^{-1}$ and $L \approx 50\,\mu m$ moves with $Re \approx .10^{-2}$. At these low values of the Reynolds number, it is justified to approximate $Re \approx 0$, for which Equation (1) is simplified to the Stokes equation

$$\nabla p = \eta \nabla^2 \boldsymbol{v}, \quad \nabla \cdot \boldsymbol{v} = 0. \tag{4}$$

Note that Equation (4) is linear and independent of time.

2.2 New meaning of Re

At very low Reynolds numbers, the motion of swimming microorganisms is dominated by viscous forces, while inertial effects are negligible. Consider a microorganism of mass m and size L swimming at velocity $\boldsymbol{V}$ in a Newtonian fluid of density ρ and viscosity η. When it stops moving, it is slowed down according to Newton's second law and eventually comes to a standstill. Since the drag force at low Reynolds number is given by $f_{\text{drag}} = ma$ and the fact that the drag force at low Reynolds number is purely viscous, $f_{\text{drag}} = -\eta V L$, $a = -\frac{VL\eta}{m}$ follows. Assuming a constant deceleration and an approximate swimmer density of $\rho_s = \frac{m}{L^3}$, the coasting distance is $d = -\frac{V^2}{2a} = \frac{\rho_s V L^2}{2\eta} = \frac{Re L \rho_s}{\rho}$. Since $\rho_s \approx \rho$ is typical, the Reynolds number has a nice interpretation: It represents the dimensionless coasting distance of a swimmer. For a human sperm cell, with $Re \sim 10^{-2}$, the stopping distance is approximately $\frac{d}{L} = 10^{-2}$, which means that the sperm cell comes to a standstill almost immediately after it has stopped moving. In contrast, a human swimmer continues to swim at a high Reynolds number due to the dominance of inertial effects. This illustrates a fundamental property of the Stokes flow: the reaction of the fluid to the boundary motion of a microswimmer is virtually instantaneous. The characteristic forces acting on the float are purely viscous and equalise at all times. Since inertial effects disappear at $Re = 0$, the total force and torque on a free-swimming microorganism must fulfil the following conditions

$$\boldsymbol{F} = 0, \quad \boldsymbol{M} = 0. \tag{5}$$

3. Rate independence and scallop theorem

The linearity and time-independence of the Stokes equation (4) are the main causes of two other properties. If we scale the speed and rotation rate of the microswimmer $\boldsymbol{V} \to \alpha \boldsymbol{V}$, $\Omega \to \alpha\Omega$, then by linearity the flow surrounding the body and the pressure scale with the same factor $\boldsymbol{v} \to \alpha \boldsymbol{v}$ and $p \to \alpha p$. The instantaneous streamlines remain identical and forces and torques also experience a similar linear scaling $\boldsymbol{F} \to \alpha \boldsymbol{F}$ and $\boldsymbol{M} \to \alpha \boldsymbol{M}$. If we were to set $\alpha = -1$, the force $\boldsymbol{F}$ and the flow $\boldsymbol{v}$ would change direction, while the flow patterns would remain identical. This postulates the *rate independence*. If a body undergoes a surface deformation, the distance travelled between two deformations depends only on the sequence of the shapes between two configurations, but not on the rate at which the surface deformation occurs.

The second property is the *scallop theorem*, which states that if the sequence of shapes displayed by the swimmer is identical in reverse time, the swimmer cannot move on average. A good example of this is a scallop. A scallop swims in such a way that it opens its shell slowly and closes it again quickly, squirting out water in the process. At a low Reynolds number, a scallop could not swim, but it has only one valve and with only one degree of freedom in configuration space, it is forced to move back and forth. The simplest animal that could swim in such a fluid is an animal with two hinges, as seen in Figure 1 [1].

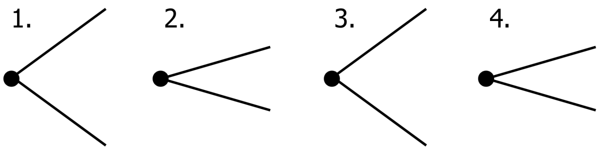

Figure 1. The swimming stroke of a scallop: This swimmer consists of two legs connected by a joint and is immersed in a viscous liquid. As the angle between the two legs changes periodically, the swimmer will move back and forth. Its net displacement, however, will be zero in the zero-Reynolds-number limit, since the swimming stroke is reciprocal. Opening the valves slowly and closing them fast is useless. Taken from Ref. [8].

4. Model of squirmer

The squirmer model is one of the canonical models for swimming with low Reynolds numbers, namely that of a writhing sphere. The microswimmer is subject to periodic deformation of a body with small amplitudes, which effectively leads to instantaneous boundary conditions on its surface. Depending on the boundary conditions, we can describe a classical translational swimmer or a squirmer with rotational motion. In our article we will focus on the former case.

4.1 Setup

Let us take the simplest example of the swimming of a spherical body with radius a. We assume that the swimmer remains spherical but exerts an instantaneous velocity field on its surface. We use a suitable spherical coordinate system with the origin at the centre of the sphere. We assume that the fluid flow is axisymmetric and therefore does not depend on the azimuthal angle, i.e., ϕ $\frac{\partial \boldsymbol{v}}{\partial \phi} = 0$. The other components of the boundary conditions are chosen arbitrarily. They lead to the swimming of a spherical body with the velocity $V(t)\boldsymbol{e}_z$ and in swimming frame the fluid flow at the infinity is

$$\boldsymbol{v}(r \to \infty) = -V(t) \cos\theta \boldsymbol{e}_r + V(t) \sin\theta \boldsymbol{e}_\theta.$$

4.2 Solution for model squirmer

We can obtain the solution for a squirmer by solving the Stokes equation, i.e. Equation (4) with the boundary conditions $v_r(a, \theta, t)$ and $v_\theta(a, \theta, t)$. Since the velocity field in the Stokes flow is biharmonic ($\nabla^2\nabla^2 \boldsymbol{v} = 0$) [5] and due to the incompressibility of the fluid $\nabla \cdot \boldsymbol{v} = 0$ we can write

$$\nabla^2\nabla^2 \left(\boldsymbol{r} \cdot \boldsymbol{v}\right) = 0, \tag{6}$$

where $\boldsymbol{r}$ is the position vector; $\boldsymbol{r} = r\boldsymbol{e}_r$. The radial component of the boundary condition is contained in this equation itself. If v_r is determined, v_θ can be found using incompressibility by explicitly integrating $\nabla \cdot \boldsymbol{v} = 0$:

$$\frac{1}{r^2}\frac{\partial}{\partial r}\left(r^2 v_r\right) + \frac{1}{r\sin\theta}\frac{\partial}{\partial \theta}\left(v_\theta \sin\theta\right) = 0.$$

To obtain all solutions of the Equation (6), we use general axisymmetric solutions of Laplace's equation $\nabla^2\Phi = 0$, which are $\Phi \sim r^n P_n(\cos\theta)$ and $\Phi \sim r^{-1-n} P_n(\cos\theta)$, where P_n is the Legendre polynomial of the n-th order [9]. To find the solution to the Equation (6), we need to solve

$$\nabla^2 \left(r v_r\right) \sim r^n P_n(\cos\theta), \quad \text{or} \quad \nabla^2 \left(r v_r\right) \sim r^{-1-n} P_n(\cos\theta).$$

Given the form of the right-hand side, we can solve the differential equation with separation of variables and look for a solution of the form $v_r(r, \theta) = f(r) P_n(\cos\theta)$. In the homogeneous part, the decaying solutions, denoted by $\tilde{\boldsymbol{v}}_{\boldsymbol{n}}$, are (since the velocity field should vanish at infinity) given by

$$\tilde{v}_{n,r} = \frac{1}{r^{n+2}} P_n(\cos\theta), \quad \tilde{v}_{n,\theta} = \frac{n}{2r^{n+2}} V_n(\theta), \quad n \geq 0, \tag{7}$$

where V_n is defined as

$$V_n(\theta) = \frac{2}{\sin\theta} \int_{\cos\theta}^{1} P_n(u)\,\mathrm{d}u = \frac{2}{n(n+1)} P_n'(\cos\theta)\sin\theta, \tag{8}$$

and where prime ($'$) denotes the derivative with respect to argument in the Legendre polynomials. The last equality is a consequence of the fact that the Legendre polynomial fulfils the Legendre differential equation [5]. The particular solution of the Equation (6) is, up to multiplicative factors, which are irrelevant due to linearity, given by

$$\bar{v}_{n,r} = \frac{1}{r^n} P_n(\cos\theta), \quad \bar{v}_{n,\theta} = \frac{1}{r^n}\left(\frac{n}{2} - 1\right) V_n(\cos\theta), \quad n \geq 1. \tag{9}$$

4.2.1 General solution

In addition to the decaying homogeneous and particular solution, the constant velocity $\hat{\boldsymbol{v}} = \boldsymbol{e}_z$ is also a solution with the components

$$\hat{v}_r = \cos\theta, \quad \hat{v}_\theta = -\sin\theta. \tag{10}$$

The solution of the Stokes flow can now be calculated exactly. The functions P_n and V_n provide a natural basis for the radial and polar components of the boundary conditions. We can write

$$v_r(a,\theta,t) = \sum_{n\geq 0} A_n(t) P_n(\cos\theta), \quad v_\theta(a,\theta,t) = \sum_{n\geq 0} B_n(t) V_n(\theta). \tag{11}$$

If the angular dependence of the boundary conditions is given in a different form than in Equation (11), Equation (11) can be inverted using standard orthogonality formulae for Legendre polynomials and the coefficients explicitly written as [5]

$$\begin{aligned}
A_n(t) &= \frac{2n+1}{2} \int_0^\pi v_r(a,\theta,t) P_n(\cos\theta)\sin\theta\,\mathrm{d}\theta, \\
B_n(t) &= \frac{1}{8} n(n+1)(2n+1) \int_0^\pi v_\theta(a,\theta,t) V_n(\theta)\sin\theta\,\mathrm{d}\theta.
\end{aligned}$$

The general form of the total solution is the linear superposition of all solutions given in the Equations (7), (9) and (10), so

$$\boldsymbol{v} = \sum_{n\geq 0} \alpha_n a^{n+2} \tilde{\boldsymbol{v}}_n + \sum_{n\geq 1} \beta_n a^n \bar{\boldsymbol{v}}_n + \Gamma \hat{\boldsymbol{v}}. \tag{12}$$

Note that the coefficients α_n, β_n, Γ generally depend on time, but for simplicity we will leave the time dependence implicit. Using the boundary conditions from Equation (11), the values of the coefficients in Equation (12) can be calculated as [5]

$$\begin{aligned}
\Gamma &= -V, \\
\alpha_0 &= A_0, \\
\alpha_1 &= \frac{1}{2}\left(2B_1 + A_1 - V\right), \\
\beta_1 &= \frac{1}{2}\left(A_1 - 2B_1 + 3V\right), \\
\alpha_n &= \left(1 - \frac{n}{2}\right) A_n + B_n, \quad (n \geq 2), \\
\beta_n &= \frac{n}{2} A_n - B_n, \quad (n \geq 2).
\end{aligned}$$

Using the fact that $P_0 = 1$, $P_1(\cos\theta) = \cos\theta$ and $V_1(\theta) = \sin\theta$, the complete solution for instantaneous flow components in the swimming frame can be written as

$$\begin{aligned} v_r(r,\theta) =& - V P_1 + A_0 \left(\frac{a}{r}\right)^2 \\ &+ \frac{1}{2}\left(2B_1 + A_1 - V\right)\left(\frac{a}{r}\right)^3 P_1 + \frac{1}{2}\left(A_1 - 2B_1 + 3V\right)\frac{a}{r}P_1 \\ &+ \sum_{n\geq 2} A_n \left[\frac{n}{2}\left(\frac{a}{r}\right)^n + \left(1-\frac{n}{2}\right)\left(\frac{a}{r}\right)^{n+2}\right] P_n \\ &+ \sum_{n\geq 2} B_n \left[\left(\frac{a}{r}\right)^{n+2} - \left(\frac{a}{r}\right)^n\right] P_n, \end{aligned} \tag{13}$$

$$\begin{aligned} v_\theta(r,\theta) =& V V_1 \\ &+ \frac{1}{4}\left(2B_1 + A_1 - V\right)\left(\frac{a}{r}\right)^3 V_1 - \frac{1}{4}\left(A_1 - 2B_1 + 3V\right)\frac{a}{r}V_1 \\ &+ \sum_{n\geq 2} \frac{n}{2}\left(\frac{n}{2} - 1\right) A_n \left[\left(\frac{a}{r}\right)^n - \left(\frac{a}{r}\right)^{n+2}\right] V_n \\ &+ \sum_{n\geq 2} B_n \left[\frac{n}{2}\left(\frac{a}{r}\right)^{n+2} + \left(1-\frac{n}{2}\right)\left(\frac{a}{r}\right)^n\right] V_n, \end{aligned}$$

where P_n and V_n denote angular functions $P_n(\cos\theta)$ and $V_n(\theta)$ respectively. Note that the term with A_0 in Equation (13) represents a source or a sink of the liquid within a sphere. For reasons of volume conservation of the swimmer, we set $A_0 = 0$.

4.3 Velocity of a squirmer

4.3.1 From general solution

We have obtained the full general solution for the Stokes flow with all required boundary conditions, but the swimming velocity V remains undetermined. The terms in the full solution that decay with $\frac{1}{r}$ actually correspond to the net force acting on the fluid. More precisely, a point force $F\boldsymbol{e}_z$ applied in the origin instantaneously generates a flow called the Stokeslet [6] with the components

$$v_r = \frac{2F}{r}P_1, \quad v_\theta = -\frac{F}{r}V_1,$$

which correspond to terms in our solution that decay with $\frac{1}{r}$. Since a squirmer moves without a net force (it must remain force-free according to Equation (5)), these terms must be set to zero, $A_1 - 2B_1 + 3V = 0$, and the swimming speed is thus given by

$$V = \frac{1}{3}\left(2B_1 - A_1\right). \tag{14}$$

As a result, the general solution simplifies to

$$\begin{aligned} v_r(r,\theta) =& -\frac{1}{3}\left(2B_1 - A_1\right) P_1 + \frac{2}{3}\left(A_1 + B_1\right)\left(\frac{a}{r}\right)^3 P_1 \\ &+ \sum_{n\geq 2} A_n \left[\frac{n}{2}\left(\frac{a}{r}\right)^n + \left(1-\frac{n}{2}\right)\left(\frac{a}{r}\right)^{n+2}\right] P_n \\ &+ \sum_{n\geq 2} B_n \left[\left(\frac{a}{r}\right)^{n+2} - \left(\frac{a}{r}\right)^n\right] P_n, \end{aligned}$$

$$
\begin{aligned}
v_\theta(r,\theta) =& \frac{1}{3}\left(2B_1 - A_1\right)V_1 + \frac{1}{3}\left(A_1 + B_1\right)\left(\frac{a}{r}\right)^3 V_1 \\
&+ \sum_{n\geq 2} \frac{n}{2}\left(\frac{n}{2} - 1\right) A_n \left[\left(\frac{a}{r}\right)^n - \left(\frac{a}{r}\right)^{n+2}\right] V_n \\
&+ \sum_{n\geq 2} B_n \left[\frac{n}{2}\left(\frac{a}{r}\right)^{n+2} + \left(1 - \frac{n}{2}\right)\left(\frac{a}{r}\right)^n\right] V_n.
\end{aligned}
$$

4.3.2 From Lorentz reciprocal theorem

In order to derive the velocity of a squirmer, we had to find a general solution for the entire Stokes flow. Stone and Samuel [10] were able to derive analytical expression relating the translational and rotational velocities of a swimmer to its arbitrary surface profile without having to solve for the entire flow field. This property of a Stokes flow is called *Lorentz reciprocal theorem*. Consider a volume of fluid V, bounded by a surface S with outward normal $\boldsymbol{n}$. The solution of Equation (4) is $\boldsymbol{v}$ (velocity of a squirmer), but here we introduce an auxiliary problem that is essential for the derivation of the reciprocal theorem. In this case, the auxiliary problem is the translation of a rigid sphere by an external force with velocity $\hat{\boldsymbol{v}}$, which is also the solution of Equation (4), and fulfils the same boundary conditions at infinity. If the stress fields of the two flows are $\boldsymbol{\sigma}$ and $\hat{\boldsymbol{\sigma}}$, then the reciprocal theorem states that:

$$
\int_S \boldsymbol{n}\cdot\hat{\boldsymbol{\sigma}}\cdot\boldsymbol{v}\ \mathrm{d}S = \int_S \boldsymbol{n}\cdot\boldsymbol{\sigma}\cdot\hat{\boldsymbol{v}}\ \mathrm{d}S.
$$

With our definition of an auxiliary problem (a translating sphere) we know the velocity of this sphere ($\hat{\boldsymbol{v}} = \hat{\boldsymbol{V}}$). Since the velocity does not depend on the surface, we can remove it from the integration so that we can use

$$
\int_S \boldsymbol{n}\cdot\hat{\boldsymbol{\sigma}}\cdot\boldsymbol{v}\ \mathrm{d}S = \int_S \left(\boldsymbol{n}\cdot\boldsymbol{\sigma}\ \mathrm{d}S\right)\cdot\hat{\boldsymbol{V}}. \tag{15}
$$

We recognize the term in the brackets as the force exerted on the body, but since free swimming occurs with no net force, as indicated in Equation (5), we know that this term is zero and the right-hand side of the equation should disappear, $\int_S \boldsymbol{n}\cdot\boldsymbol{\sigma}\ \mathrm{d}S = 0$. The Equation (15) simply becomes

$$
\int_S \boldsymbol{n}\cdot\hat{\boldsymbol{\sigma}}\cdot\boldsymbol{v}\ \mathrm{d}S = 0. \tag{16}
$$

The surface velocity of an original squirmer problem is then decomposed into the unknown translational squirmer velocity $\boldsymbol{V}$ and the arbitrary surface squirming motion $\boldsymbol{v'}$ so that $\boldsymbol{v}(S) = \boldsymbol{V} + \boldsymbol{v'}$. With these boundary conditions, Equation (16) can be rewritten as

$$
\left(\int_S \boldsymbol{n}\cdot\hat{\boldsymbol{\sigma}}\ \mathrm{d}S\right)\cdot\boldsymbol{V} = -\int_S \boldsymbol{n}\cdot\hat{\boldsymbol{\sigma}}\cdot\boldsymbol{v'}\ \mathrm{d}S. \tag{17}
$$

To determine translational velocity of a squirmer, we need to evaluate both integrals. To solve them, some knowledge of the auxiliary stress field is required. As can be seen in Equation (3), the integral on the left-hand side represents the Stokes drag force of a rigid sphere, which can be expressed as $\hat{\boldsymbol{F}} = \int_S \boldsymbol{n}\cdot\hat{\boldsymbol{\sigma}}\ \mathrm{d}S = -6\pi\eta a\hat{\boldsymbol{V}}$. In particular, for a sphere with the radius a, the surface stress is $\boldsymbol{n}\cdot\hat{\boldsymbol{\sigma}} = -\frac{3\eta}{2a}\hat{\boldsymbol{V}}$ [10]. It follows that Equation (17) becomes

$$
-6\pi\eta a\hat{\boldsymbol{V}}\cdot\boldsymbol{V} = \frac{3\eta}{2a}\hat{\boldsymbol{V}}\cdot\int_S \boldsymbol{v'}\ \mathrm{d}S,
$$

which finally gives us a formula for the velocity of a squirmer

$$\boldsymbol{V} = -\frac{1}{4\pi a^2}\int_S \boldsymbol{v'}\,\mathrm{d}S. \tag{18}$$

Note that we have obtained the swimming velocity of a squirmer $\boldsymbol{V}$ as a simple surface integral of its surface motion $\boldsymbol{v'}$, without actually solving for the flow field around the swimmer. However, some knowledge of an auxiliary stress field is required, which means that flow calculations had to be performed at some point. The Equation (18) is not only valid for a stationary Stokes flow, but also applies to time-dependent cases in which $\boldsymbol{v'}$ then represents the instantaneous surface velocity. The mean swimming velocity then corresponds to the time average of the equation.

Above, we have written a formula for the velocity of a squirmer based only on the velocity at the surface of the swimmer. Let us evaluate it. By assuming spherical shape of a squirmer with radius a, we write $\mathrm{d}S = a^2 \sin\theta\,\mathrm{d}\theta\,\mathrm{d}\phi$. It is also known that the surface velocity is axisymmetric and does not depend on ϕ, i.e. $\mathrm{d}S = 2\pi a^2 \sin\theta\,\mathrm{d}\theta$. Due to the axisymmetry, the velocity is expected to be directed along the z axis, so we also project the Equation (18) onto the z axis to obtain an integral for the swimming velocity $\boldsymbol{V}$ as

$$\boldsymbol{V} = -\frac{1}{2}\int_0^\pi \boldsymbol{v'}(a,\theta)\boldsymbol{e}_z \sin\theta\,\mathrm{d}\theta, \tag{19}$$

where the surface velocity $\boldsymbol{v'}$ is given by the boundary conditions in Equation (11). If we insert Equation (11) into Equation (19) and $\boldsymbol{v'}\boldsymbol{e}_z = v_r\cos\theta - v_\theta \sin\theta$, we get

$$\boldsymbol{V} = \frac{1}{2}\sum_{n\geq 1} B_n \int_0^\pi \sin^2\theta V_n(\theta)\,\mathrm{d}\theta - \frac{1}{2}A_n\int_0^\pi \sin\theta\cos\theta P_n(\cos\theta)\,\mathrm{d}\theta. \tag{20}$$

Using the orthonogality property of the Legendre polynomials [5] and considering the definition of V_n from Equation (8) together with the fact that $P_1 = \cos\theta$, we see that all integrals in Equation (20) vanish except for the terms $n = 1$, which leads us to

$$\boldsymbol{V} = \frac{1}{2}B_1\int_0^\pi \sin^3\theta\,\mathrm{d}\theta - \frac{1}{2}A_1\int_0^\pi \sin\theta\cos^2\theta\theta\,\mathrm{d}\theta = \frac{1}{3}\left(2B_1 - A_1\right),$$

which corresponds to the velocity we obtained from the full solution of the Stokes flow – Equation (14). Note that the velocity depends on the first mode of each surface velocity component in the boundary condition defined in Equation (11), but not on the viscosity of the fluid, since thrust and drag scale linearly at $Re \approx 0$ [11].

4.4 Pusher – puller

We introduce a reduced-order squirmer with the assumption that the surface deforms uniformly and only in the tangential direction ($A_n = 0$ and $B_n = constant$). Furthermore, we assume $B_n = 0$ for $n \geq 3$, since B_1 and B_2 already capture the essential and dominant feature of the free-swimming squirmer, so that the surface velocity is [4]

$$\boldsymbol{v}_S(\theta) = B_1\sin\theta + B_2\sin\theta\cos\theta.$$

The first term is solely responsible for the propulsion (since $A_n = 0$), $\boldsymbol{V} = \frac{2}{3}B_1$, and generates an irrotational velocity field, that decays with $\frac{1}{r^3}$. In the laboratory frame, the velocity field generated by the term B_1 is therefore

$$\boldsymbol{v}_{B_1}(r,\theta) = \frac{a^3}{3r^3}B_1\left(2\cos\theta\boldsymbol{e}_r + \sin\theta\boldsymbol{e}_\theta\right),$$

which physically corresponds to the potential source dipole in the Stokes flow (where the Reynolds number is effectively zero). The term with B_2 generates a velocity field

$$\boldsymbol{v}_{B_2}(r,\theta) = -\frac{B_2 a^2}{4r^2}(1+3\cos 2\theta)\boldsymbol{e}_r + \frac{B_2 a^4}{4r^4}\left[(1+3\cos 2\theta)\boldsymbol{e}_r + 2\sin 2\theta \boldsymbol{e}_\theta\right].$$

This velocity field is called the Stresslet and describes how squirmer moves the fluid without applying a net force. Its lowest decaying term decays as $\frac{1}{r^2}$. A velocity field generated exclusively by the B_1 mode corresponds to a potential dipole. In contrast, the B_2 mode generates a Stokes dipole flow that decays with $\frac{1}{r^2}$ and is characterised by a purely radial movement. Negative values of B_2 correspond to inward-directed dipoles, while positive values correspond to outward-directed dipoles. A positive dipole represents two opposing forces pushing away from each other, whereas a negative dipole has forces pulling toward each other. These force dipoles do not exert a net force on the surrounding fluid. To characterise the swimming mechanism more generally, we introduce the squirmer parameter β, defined as $\beta = \frac{B_2}{B_1}$, where B_1 is always positive. This parameter distinguishes between two types of swimmers: *pushers* ($\beta < 0$) and *pullers* ($\beta > 0$). Pushers, such as *E. coli* and flagellated sperm, generate thrust from behind, expelling fluid along their swimming direction while drawing it in from the sides. Pullers, such as *Chlamydomonas*, rely on thrust from the front, attracting fluid along their swimming axis and expelling it laterally. When both B_1 and B_2 modes are present, the total flow field combines propulsion with the characteristic dipolar signature, producing the distinct patterns associated with pushers and pullers.

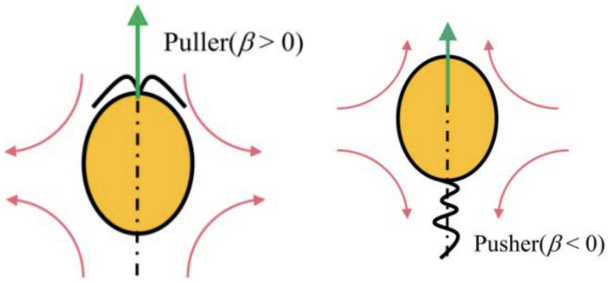

Figure 2. Picture of two swimmers relying on two different mechanisms. Puller (upper) generate thrust in front of them in direction of swimming, pusher (lower) generate thrust behind them. Squirmers are force-free swimmers since thrust and drag effectively cancel each other out. Taken from Ref. [12].

5. Motion of a single squirmer near a wall

In this section, we analyse the movement of a single squirmer near a no-slip boundary. The squirmer is considered at a distance h from the wall, with an orientation angle α. The wall is located at $y = 0$, and the squirmer moves in the x-y plane. Numerical simulations reported in Ref. [13] show that when a squirmer approaches a wall it first collides with the boundary and then moves along it for a certain period of time, the so-called *contact time*, before eventually swimming away. The contact time is found to decrease with increasing squirmer parameter β. Based on the results of Ref. [13], three distinct swimming behaviours can be identified depending on β:

1. For $\beta \leq 1$, the squirmer escapes from the wall at a positive angle.

2. For $2 \leq \beta \leq 5$, the squirmer oscillates near the boundary before eventually settling into a stable parallel trajectory at a fixed distance. Cases with $\beta = 4.5$ exhibit weak damping, leading to persistent oscillations.

3. For $\beta \geq 7$, the squirmer follows a cyclical trajectory and repeatedly bounces off the wall. The oscillation amplitude remains small in relation to the wavelength.

Furthermore, Ref. [13] shows that for squirmers that eventually move away from the wall ($\beta \leq 1$), the steady-state swimming speed decreases as β increases. This is consistent with analytical results for inertial squirmers in unconfined regions [14]. In contrast, pullers ($\beta > 2$) tend to remain close to the wall, with their swimming speed increasing with increasing β. Swimming along boundaries is particularly important for certain microswimmers, such as spermatozoa, whose pusher-like flow fields ($\beta < 0$) stabilise motion near walls without leading to the kind of trapping behaviour observed for pullers [15].

6. Comparison with experiment: Volvox

To conclude this article, we compare the theoretical predictions of the squirmer model with experimental observations. We focus on the green alga *Volvox carteri*, a multicellular, almost spherical organism that serves as a model system in biological hydrodynamics. The surface of *Volvox carteri* is covered with thousands of small somatic cells, each carrying a pair of flagella that protrude into the surrounding fluid. These flagella beat in a coordinated manner, creating a fluid flow and propelling the organism. In reality, *Volvox* appears as a nearly spherical colony, with the flagellated cells evenly distributed on its surface. Experimental measurements of the time-averaged flow generated by the flagella, carried out using particle image velocimetry, show that when the alga is held in place by a pipette the surrounding flow resembles that of the squirmer model described in Sections 4.2–4.3. Because the organism is not free-swimming but fixed, it exerts a net force on the fluid, which gives rise to a long-range $1/r$ decay mode in the velocity field. If both the force and Stresslet contributions are included and higher-order terms neglected, the velocity components of the squirmer model take the form:

$$v_r(r,\theta) = B_1 \left[\left(\frac{a}{r}\right)^3 - \frac{a}{r} \right] \cos\theta + \frac{B_2}{2} \left[\left(\frac{a}{r}\right)^4 - \left(\frac{a}{r}\right)^2 \right] \left(3\cos^2\theta - 1\right),$$

$$v_\theta(r,\theta) = \frac{B_1}{2} \left[\left(\frac{a}{r}\right)^3 + \frac{a}{r} \right] \sin\theta + B_2 \left[\left(\frac{a}{r}\right)^4 \right] \sin\theta\cos\theta.$$

A best-fit analysis between the experimental velocity field and the theoretical prediction indicates that the optimal value of the squirmer parameter is $\beta = 0.1$. This two-mode squirmer model reproduces the key experimental features: a slight asymmetry of the flow from front to back, the strongest velocities located near the equator of the colony, and the overall structure of the flow induced by the flagellar beating on the spherical surface of the alga.

7. Conclusion

Through the squirmer model, we have gained valuable insights into the basic principles of microswimmer locomotion at low Reynolds numbers. We have explored how self-propulsion arises from surface distortions, how different types of motion define pushers and pullers, and how these swimmers interact with boundaries. Importantly, the model captures key features of real biological systems, such as Volvox carteri, and provides predictions that are consistent with experimental observations. The squirmer model effectively bridges theory and biology, and provides a powerful framework for understanding and predicting the behaviour of microswimmers in complex fluid environments.

REFERENCES

[1] E. M. Purcell, *Physics and our world: reissue of the proceedings of a symposium in honor of Victor F Weisskopf*, World Scientific 2014, 47.

[2] M. J. Lighthill, *On the squirming motion of nearly spherical deformable bodies through liquids at very small reynolds numbers*, Communications on pure and applied mathematics **5** (1952), 109.

[3] J. R. Blake, *A spherical envelope approach to ciliary propulsion*, Journal of Fluid Mechanics **46** (1971), 199.

[4] O. S. Pak and E. Lauga, *Theoretical models of low-reynolds-number locomotion*, Royal Society of Chemistry, London, 2014.

[5] E. Lauga, *The fluid dynamics of cell motility, Vol. 62*, Cambridge University Press, Cambridge, 2020.

[6] J. Happel and H. Brenner, *Low reynolds number hydrodynamics, mechanics of fluids and transport processes*, Martinus Nijhoff Publishers, Leiden, 1973.

[7] E. Lauga and T. R. Powers, *The hydrodynamics of swimming microorganisms*, Reports on progress in physics **72** (2009), 4.

[8] B. Friedrich, *Chemotaxis of Sperm Cells*, Ph.D. thesis, Fakultät für Mathematik und Naturwissenschaften Technische Universität Dresden, 2009.

[9] K. F. Riley, M. P. Hobson, and S. J. Bence, *Mathematical methods for physics and engineering*, Cambridge University Press, Cambridge, 1921.

[10] H. A. Stone and A. D. Samuel, *Propulsion of microorganisms by surface distortions*, Physical Review Letters **77** (1996), 1.

[11] N. G. Chisholm, D. Legendre, E. Lauga, and A. S. Khair, *A squirmer across reynolds numbers*, Journal of Fluid Mechanics **796** (2016), 233.

[12] G. Guan, J. Lin and D. Nie, *Swimming Mode of Two Interacting Squirmers under Gravity in a Narrow Vertical Channel*, Entropy **24** (2022), 1.

[13] G.–J. Li and A. M. Ardekani, *Hydrodynamic interaction of microswimmers near a wall*, Physical Review E **90** (2014), 1.

[14] S. Wang and A. Ardekani, *Inertial squirmer*, Physics of Fluids **24** (2012), 3.

[15] J. Elgeti, U. B. Kaupp, and G. Gompper, *Hydrodynamics of sperm cells near surfaces*, Biophysical journal **99** (2010), 1018.